Interference in Wireless Multihop Networks: A Model and its Experimental Evaluation

Georgios Parissidis, Merkourios Karaliopoulos, Martin May, Thrasyvoulos Spyropoulos, Bernhard Plattner
Computer Engineering and Networks Laboratory
ETH Zurich, Switzerland
{parissid,karaliopoulos,may,spyropoulos,plattner}@tik.ee.ethz.ch

Abstract

Interference is an inherent property of wireless multihop networks. Adding interference-awareness to their control functions can significantly enhance the overall network performance. In this paper we present an analytical model for the probability that a transmission destined to an arbitrary network node is successful in the presence of interference from other nodes in the network. We introduce the concept of interference areas *and* interference zones *to express this probability as a function of the network density, node transmission probability, radio propagation environment, and network card reception sensitivity. Our derivation includes a simple MAC model, which captures the carrier sense function of many MAC protocols. Contrary to measurement-based models, our derivation only requires information that is locally available to the nodes, avoiding all measurement-related pitfalls. The validation of our model against experiments in a real testbed, set up for this purpose in our indoor office environment, shows good match of the experimental results with the analytical predictions. Interestingly our model predictions follow closely those of more elaborate state-of-the-art analytical models. Finally, to demonstrate the real utility of our model, we have implemented on our testbed a routing metric that explicitly takes interference into account via our derivation. The throughputs of the resulting routes compare favorably with those achieved by a well-known probe-based routing metric.*

1 Introduction

The standardization of Wireless Local Area Networks (WLANs) [1] opened the way to wireless network access provision without the need for wired infrastructure. The IEEE 802.11 ad hoc mode, in particular, enabled the intercommunication of mobile, battery-powered devices and opened the way to a revolutionary method of communication that departs from the well-established infrastructure-based network access paradigm. In this new paradigm, messages are routed (relayed) over multiple wireless (*mesh*) hops to reach their destination.

Yet, within this paradigm, interference becomes a major impact factor on the network efficiency and performance. Due to the broadcast nature of the medium and the complexity of wireless propagation phenomena it is inherently difficult to spatially partition the wireless medium into clearly disjoint links as in the case of wired networks. This, combined with the random access nature (implemented by a carrier sense function) of the 802.11 MAC protocol gives rise to nodes that *do* transmit while they *shouldn't* (hidden nodes) but also nodes that *do not* transmit while they *could* (exposed nodes). Both phenomena result in significant reduction of the information delivery capacity of the network.

Adding interference-awareness to routing decisions can therefore enhance significantly the network performance. Jain *et al.* in [2] show that under ideal interference-aware routing, the data delivery capability of the network can be significantly improved with respect to shortest-path routing, even under non-optimal MAC scheduling. Nevertheless, almost all routing metrics proposed in the literature as alternatives to minimum-hop metrics do not explicitly account for interference (see, for example, [3] and [4]). They are rather measurement-based estimates of higher-level metrics of network performance, such as delay or number of retransmissions, that do partly depend on interference but capture its effect indirectly. Measurement-based approaches have two major disadvantages. The first one is the data overhead they impose on the network. The second one has to do with the achievable accuracy and reliability of the measurements. For example, getting an estimate for a link loss of $x\%$ would require the availability of around $1000/x$ measurement samples, *i.e.*, packets, as a rule of thumb. This clearly does not scale for small to moderate error rates, even when measurements are carried out via broadcast packets.

These considerations motivated us to take a different approach. We would like to answer the following question:

how well can we estimate interference and predict the success probability of transmitting a message over a link without resorting to measurements and probing, but rather by exploiting only information that is locally available to the node? In other words, we would like to come up with a simple yet accurate analytical metric for the probability of successful transmission over each link, that can be used by an interference-aware routing protocol to choose routing paths that maximize throughput.

To this end, we develop an analytical model to estimate the probability that a transmission destined to node is successful in the presence of interference from other nodes in the network. Starting from the simple physical (SINR) model [5], we introduce the concepts of *interference areas* and *interference zones* with respect to the intended data recipient node; these zones aim at quantifying the effect of cumulative interference by concurrently transmitting nodes outside the immediate neighborhood of a node. Furthermore, to also capture the carrier sense function of many MAC protocols we include in our model a very simple and generic MAC model, which ensures that nodes within range of the transmitting source defer from transmitting. Accounting for both these effects, we derive an analytical expression for the probability of successful reception in the presence of interference, as a function of the node degree, node transmission probability, radio propagation environment, and network card reception sensitivity. Compared to probe-based approaches, the advantage of this derivation is that all model inputs can be available (or estimated) locally to the node; for example, information regarding a node's degree can be extracted from the routing layer at no additional cost in terms of communication overhead. Compared to other, more complex analytical models of wireless interference [6, 7], our model does not require prior measurements and can scale up to large number of nodes. Interestingly, its simplicity comes without significant loss in prediction accuracy, as our evaluation of the model suggests.

Nevertheless, our analytical model does not capture the exact working details of a realistic 802.11 protocol (*e.g.*, Distributed Coordination Function of 802.11 [1]), and also unavoidably makes some assumptions with respect to real propagation phenomena, in order to ensure it remains simple enough to be utilized as a handy routing metric. To evaluate the effect of our assumptions in a real world setting, we validate our model against experiments in a real testbed, set up for this purpose in our indoor office environment. Despite the generic nature of the model, the experimental results from our IEEE 802.11 testbed show good match with the analytical predictions, and advocate the model's utility for real-world MAC protocols and realistic radio propagation conditions. We find that our model predictions follow closely those of more elaborate well-known analytical models [7]. Finally, to demonstrate the real utility of our model, we have implemented on our testbed a routing metric that explicitly takes interference into account via our derivation. The throughputs of the resulting routes compare favorably with those achieved by a well-known probe-based routing metric [3].

The paper is organized as follows. In Section 2, we present our analytical derivation for the probability of successful reception in the presence of interference. We devote Section 3 to numerical results showing the model sensitivity to its parameters and their independencies. The model validation against testbed experiments is carried out in Section 4. In the same section we compare our model predictions with those made by other models and present its utility as routing metric. We summarize related work in Section 5 and conclude the paper with a discussion on future directions in Section 6.

2 Analytical model

Our analytical model formulation proceeds as follows. First, we derive the probability of successful reception $P(x_j)$ at a receiver node x_j in the presence of *cumulative interference* for a "MAC-agnostic" model, where nodes do not sense the medium before transmitting. Then, we include a simple enhancement into our model that aims at capturing the effect of carrier sense and calculate $P(x_j)$ for the complete model. Central to our derivation is the concept of *interference zone*, which aims at quantifying the effect of cumulative interference by multiple concurrently transmitting nodes at various "distance zones" away from the receiver. Finally, we show how this probability can be expressed as a function of radio and propagation parameters, node degree, and network load.

2.1 Physical model and assumptions

In our analysis, the network comprises a set of nodes $X = \{x_1, .., x_n\}$ located in the Euclidean plane. The reference physical model that determines whether a packet is received successfully or not is the Signal-to-Interference-Noise-Ratio (SINR) model (see, for example [5]). Under the SINR model, the transmission success depends on the received signal strength, the interference caused by simultaneously transmitting nodes, and the environmental noise level. Let $P_{w,i}$ be the transmit power of node i, and T the set of nodes transmitting at that instant ($T \subseteq X$). A transmission from node $x_i, i \in T$, is successfully received by node x_j if

$$\frac{\frac{P_{w,i}}{|x_i - x_j|^\alpha}}{N + \sum_{k \in T, k \neq i} \frac{P_{w,k}}{|x_k - x_j|^\alpha}} \geq \beta. \quad (1)$$

Table 1. A summary of key notation

α	Path loss exponent
β	SINR threshold
γ	Transmission probability
r	Euclidean distance between sender x_i and receiver x_j
P_w	Transmit power
N	Thermal noise
$P(x_j)$	Probability of successful delivery at node x_j
$C_{j,m}$	m^{th} interference area with respect to recipient node x_j
$r_{j,m}$	radius of m^{th} interference area $C_{j,m}$
$A_{j,m}$	m^{th} interference zone with respect to recipient node x_j
$n(A_{j,m})$	Number of nodes in interference zone m
M	Maximum number of interference zones
ρ	Node density

In Eq. (1) $|x_i - x_j|$ denotes the Euclidean distance between nodes x_i and x_j and N is the ambient noise power level. The parameter α is the path loss exponent, which depends on the environment and typically ranges from 2 to 5. The SINR model implies that a minimum signal-to-interference ratio of β is necessary for successful reception. The actual value of β primarily relates to the specific physical layer design, such as the deployed modulation, interleaving, and coding schemes.

For the sake of analytical tractability, we make the following set of assumptions:

A.1 All nodes have similar receiver chain characteristics: omnidirectional antenna, the same transmit power and noise floor, and similar physical layer performance, i.e., $P_{w,i} = P_{w,j} = P_w$ and $\beta_i = \beta_j = \beta \, \forall i \neq j$. This is called the *uniform node* assumption. Given this, the maximum distance r_{max} for successful signal reception is given from

$$r_{max} = |x_i - x_j|_{max} = \sqrt[\alpha]{\frac{P_w}{N \cdot \beta}}. \qquad (2)$$

A.2 Nodes transmit with equal probability γ (*uniform load* assumption). The probability γ reflects the uniform network load [8], [9].

In Table 1 we summarize our notation.

2.2 Interference ("MAC-agnostic") Model

We first assume that all nodes access the medium without previously checking to see if any other node is already transmitting nearby, and evaluate the effect of cumulative interference on message reception for an arbitrary sender-receiver pair. This simple model, sometimes referred to as *physical model* [5], has often been used in studies of network throughput for ad hoc networks. Here, in order to better quantify the additive effect of interfering nodes at different distances from the intended receiver, we introduce the concept of *interference zones*.

DEFINITION 1. An interference zone $A_{j,m}$ with respect to a receiver node x_j is the area over which a **minimum** of m simultaneous transmissions result in unsuccessful reception at node x_j.

LEMMA 1. Assuming that a node x_i transmits to another node x_j at distance r. Then, a third node x_k lies in the interference zone $A_{j,m}$ of $x_j, m \in \{1, 2, 3...\}$, if its Euclidean distance to the intended recipient node x_j is

$$\sqrt[\alpha]{(m-1)\beta} \cdot r < |x_k - x_j| \leq \sqrt[\alpha]{m\beta} \cdot r, \quad m \in \{1, 2, 3...\} \qquad (3)$$

Proof. From (1) and assumption A.1, the simultaneous transmission of m nodes will not result in unsuccessful reception due to interference at node x_j, as long as

$$\frac{\frac{P_w}{r^\alpha}}{N + \sum_{k=1, k\neq i}^{m} \frac{P_w}{|x_k - x_j|^\alpha}} \geq \beta.$$

Assuming that noise N is sufficiently small comparing to the interference induced from the simultaneous transmissions[1], it follows that

$$\frac{P_w}{r^\alpha} \geq (\sum_{k=1, k\neq i}^{m} \frac{P_w}{|x_k - x_j|^\alpha})\beta.$$

The sum on the right hand side is maximized when the distance $|x_k - x_j|$, $\forall \, x_k \in A_{j,m}$ is minimized. Requiring that

$$\frac{P_w}{r^\alpha} \geq \left(\sum_{k=1, k\neq i}^{m} \frac{P_w}{|x_k - x_j|_{min}^\alpha}\right)\beta$$

we get

$$\frac{P_w}{r^\alpha} \geq \frac{m \cdot P_w}{|x_k - x_j|_{min}^\alpha}\beta.$$

Therefore,

$$|x_k - x_j|_{min}^\alpha \geq m\beta \cdot r^\alpha$$
$$|x_k - x_j|_{min} \geq \sqrt[\alpha]{m\beta} \cdot r \equiv r_{j,m}.$$

In other words, the simultaneous transmission of m nodes will not result in unsuccessful reception due to interference at node x_j, if all m nodes lie at distance greater than $\sqrt[\alpha]{m\beta} \cdot r$ and vice versa.

We use the notation $C_{j,m}$ for the area within the circle of radius $\sqrt[\alpha]{m\beta} \cdot r$, hereafter called *interference area*; then, $\overline{C_{j,m}}$ denotes the area outside that circle. At least

[1] Thermal noise N for a 2.4GHz channel as used in wireless networks is very small compared to the interference.

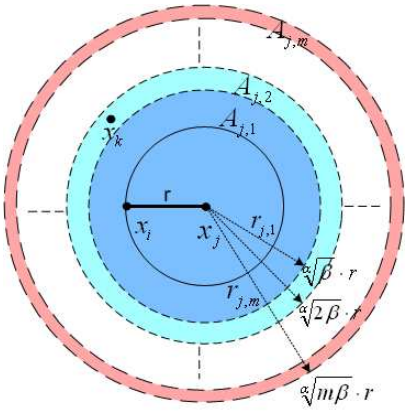

Figure 1. Interference zones $A_{j,m}$ with respect to recipient node x_j

$m+1$ nodes are required in $\overline{C_{j,m}}$, even when all of them are placed at the minimum possible distance $r_{j,m}$ from the receiving node, to prevent the successful delivery of the packet. Then, the interference zone $A_{j,m}$ is the intersection of interference area $C_{j,m}$ with the complement of interference area $C_{j,m-1}$, $C_{j,m} \bigcap \overline{C_{j,m-1}}$, as shown in Fig. 1. For example, a node x_k is located in the interference zone $A_{j,2}$ if its Euclidean distance to node x_j is $\sqrt[\alpha]{\beta} \cdot r < |x_k - x_j| \leq \sqrt[\alpha]{2\beta} \cdot r$. □

We now estimate $P(x_j)$, the probability that a transmission destined to node x_j is successful despite interference from any other nodes in the network.

THEOREM 1. Under the assumptions A.1-A.2, the probability $P(x_j)$ is given by

$$P(x_j) = (1-\gamma)^{n(A_{j,1})} \sum_{i_2=0}^{1} \binom{n(A_{j,2})}{i_2} \gamma^{i_2} (1-\gamma)^{n(A_{j,2})-i_2} \sum_{i_3=0}^{2-i_2} \binom{n(A_{j,3})}{i_3} \gamma^{i_3} (1-\gamma)^{n(A_{j,3})-i_3} \cdots \sum_{i_M=0}^{M-1-\sum_{n=1}^{M-1} i_n} \binom{n(A_{j,M})}{i_M} \gamma^{i_M} (1-\gamma)^{n(A_{j,M})-i_M} \quad (4)$$

where γ is the probability that a node is transmitting at the MAC layer, $n(A_{j,m})$ are the number of nodes in interference zone $A_{j,m}$ and M corresponds to the number of interference zones $A_{j,m}$ $m \in \{1, 2, 3...\}$ that are taken into account.

Proof. In the light of Definition 2, to avoid destructive interference at the receiver node x_j, the number of nodes in each interference area $C_{j,m}$ $m \in \{1, 2, ..M\}$ should not exceed $m-1$. The allowed number of transmissions within each interference zone is strongly dependent on the ongoing transmissions in the other interference zones. Apparently there is an area, the first interference zone $A_{j,1}$, which coincides with $C_{j,1}$, where no transmission should happen. Likewise, up to one transmission can be tolerated in interference zone $A_{j,2}$, whereas the transmissions i_3 in zone $A_{j,3}$ should definitely not exceed two but could be further restricted to one, if there is simultaneous transmission in zone $A_{j,2}$. Iterative application of the same argument results in Eq. (4). □

The number M of interference zones that are taken into account in this equation is dependent on the node spatial distribution. In paragraph 2.4 we get numerical values for M when nodes are uniformly distributed in space.

The node transmission probability γ is a measure of the traffic load input to the network. Note that γ represents the per-node traffic load that appears at the wireless medium after the MAC protocol shaping, rather than the higher-layer packet transmission rate. In general, the parameter γ and the number of nodes competing for the medium are coupled with each other, *i.e.*, they do not vary independently. Their exact coupling relationship differs according to the details of the specific MAC protocol. In the IEEE 802.11x suite of protocols, for example, it is well known that the actual allowed values of the transmission probability γ depend on many parameters such as the number of contending nodes, the back-off algorithm, and the bandwidth of the wireless medium (see [8] and [9]). In section 6 we discuss how we can estimate the parameter γ in an IEEE 802.11x protocol and then use it in Eq. (4).

2.3 Interference-cum-MAC Model

In this section we extend our model to capture essential properties of CSMA MAC protocols. The "MAC-agnostic" interference model overestimates the cumulative interference because it assumes that nodes can transmit independently. However, in CSMA MAC protocols nodes defer when they sense the medium busy (when the reception energy is over the *Clear Channel Assessment* threshold, CCA_{thr}) and schedule a transmission based on an exponential backoff algorithm. This mechanism only partially solves the problem of interfering transmissions as often nodes within the interference range of the receiver are outside the carrier sense range of the sender (hidden nodes problem). To keep our model simple, rather than incorporating the full complexity of CSMA MAC protocols, we include in our model a simple generic MAC that takes into account the physical carrier sense property (CCA_{thr}) for the nodes located in the first interference zone $A_{j,1}$. In other words, all nodes within carrier sense range from the transmitter and inside the first interference zone of the receiver defer from transmitting. Whereas this is only an approximation, our evaluation shows that this enhancement already

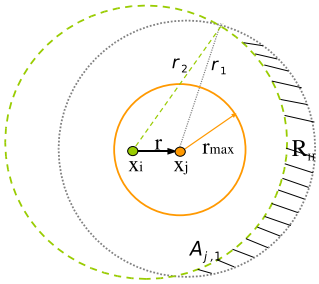

Figure 2. Hidden nodes area R_H in the first interference zone $A_{j,1}$

has sufficient power to predict the successful packet reception probability under unsaturated demand.

In Figure 2, $r_1 = \sqrt[\alpha]{\beta} \cdot r$ denotes the radius of interference zone $A_{j,1}$ and $r_2 = \sqrt[\alpha]{\frac{Pw_i}{10^{CCA_{thr}/10}}} = (1+\epsilon) \cdot r_1$ is the sender's physical carrier sense range. Hidden nodes can still exist in the area R_H, given by

$$S_{R_H} = \pi r_1^2 - B \tag{5}$$

where B is the surface of the intersection between $A_{j,1}$ and sender's physical carrier sensing area [10], given by

$$\begin{aligned} B &= r_1^2 cos^{-1}\left(\frac{r^2+r_1^2-r_2^2}{2\cdot r\cdot r_1}\right) + r_2^2 cos^{-1}\left(\frac{r^2+r_2^2-r_1^2}{2\cdot r\cdot r_2}\right) \\ &- \frac{1}{2}\sqrt{(r_1+r_2-r)(r_1+r_2+r)(r_1-r_2+r)(r_2-r_1+r)} \end{aligned} \tag{6}$$

The probability of successful reception $P(x_j)$ for the complete model results from Eq. (4) when replacing $n(Aj,1)$ with $n(R_H)$. In the rest of the paper we use the probability of successful reception $P(x_j)$ obtained from the *Interference-cum-MAC* model.

2.4 Probability of Successful Reception under Uniform Node Distribution

The probability of successful reception at a node x_j, is a function of the network load (γ), number of network nodes $n(A_{j,m})$ in each interference zone $A_{j,m}$, $\forall\, m \in \{1,2,3...\}$, propagation environment (α), and hardware equipment (β). Note that the formula can address both static and mobile networks in contrast with other models that apply only to static networks [6, 7]. In the second case, the requirement is the existence of a steady-state spatial node distribution as a result of the node mobility patterns. Bettstetter *et al.* , for example, have derived analytically this distribution for the random waypoint (RWP) mobility model in [11]. Their result could be directly used to derive the number of nodes per interference zone, $n(A_{j,m})$, whenever the RWP model is deemed a valid assumption for the node mobility.

It would be desirable to express the probability of successful reception $P(x_j)$ as a function of network density and particularly the node degree, as this is a quantity that can be obtained locally. We achieve this, assuming uniform node distribution. Note that this is the distribution resulting from a range of mobility models widely used in literature such as the random walk and random direction [12] models.

For each node x_i it is possible to define its node degree and transmission range.

DEFINITION 2. The node degree $d(x_i)$ of a node x_i is

$$d(x_i) = |\{x_j | \frac{\frac{P}{|x_i - x_j|^\alpha}}{N} \geq \beta, x_j \in X \setminus \{x_i\}\}|. \tag{7}$$

In other words, the degree of the node x_i equals the number of network nodes from which x_i can successfully receive a signal in the absence of any interference from other nodes. In the case of uniform node distribution with node density equal to ρ, it is easy to see that

$$d(x_i) = \rho\pi(r_{max})^2. \tag{8}$$

Throughout the rest of the paper, we are going to assume that the node degree is manipulated *independently of other parameters* by changing the corresponding node density.

Under the uniform node assumption, the expected number of nodes in an interference zone $A_{j,m}$ will be proportional to its surface

$$E[n(A_{j,m})] = \frac{\pi\sqrt[\alpha]{(m\beta)^2}\cdot r^2}{A}n - \frac{\pi\sqrt[\alpha]{\left((m-1)\beta\right)^2}\cdot r^2}{A}n$$

where $r = |x_i - x_j|$ is the transmitter-receiver distance. The latter is always a function of the maximum communication range r_{max}

$$r = c \cdot r_{max}. \tag{9}$$

where $0 < c < 1$, a scale factor that depends on the node distribution but also the routing protocol. For example, minimum-hop routing protocols tend to select nodes at the edge of coverage as next-hop, implying a value of c close to unity. On the contrary, protocols that favor reliable over shortest paths will yield smaller values of c. $E[n(A_{j,m})]$ can now be written as a function of the node degree $d(x_j)$

$$E[n(A_{j,m})] = c^2 \cdot \left(\sqrt[\alpha]{(m\beta)^2} - \sqrt[\alpha]{[(m-1)\beta]^2}\right) \cdot d(x_j) \tag{10}$$

We can then write the probability $P(x_j)$ as a function of the node degree $d(x_j)$, if we replace $n(A_{j,m})$ in Eq. (4) with $E[n(A_{j,m})]$, rounded to the closest integer, for the expected number of nodes in interference zone $A_{j,m}$.

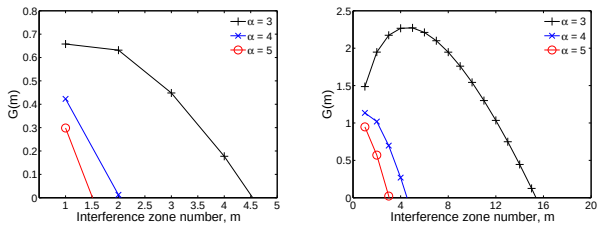

(a) $\beta = 2.5, c = 0.3, d(x_j) = 10$ (b) $\beta = 2.5, c = 0.3, d(x_j) = 15$

Figure 3. $G(m)$ **as a function of the number** m **of interference areas/zones for given** α, β, c**, and** $d(x_j)$

2.4.1 Interference zone number estimation

The number of nodes in all circles $C_{j,m},\ m \in \{1, 2, ..M\}$ should be greater than the number of potential senders,

$$G(m) = \sum_{i=1}^{m} E[n(A_{j,m})] - m \geq 0 \qquad (11)$$

Given Eq. (10), $G(m)$ is written

$$\begin{aligned} G(m) &= \sum_{i=1}^{m} c^2 \cdot \left(\sqrt[\alpha]{(i\beta)^2} - \sqrt[\alpha]{[(i-1)\beta]^2} \right) \cdot d(x_j) - m \\ &= c^2 \cdot \sqrt[\alpha]{(m\beta)^2} \cdot d(x_j) - m, \end{aligned} \qquad (12)$$

where $2 \leq \alpha \leq 5$, $\beta > 0$, $d(x_j) > 0$. Then the number M of interference zones can be defined as

$$M = max\{m | G(m) \geq 0\ ,\ m \in \{1, 2, 3, ...\}\ \} \qquad (13)$$

The parameter M can be computed only numerically for given α, β, c, and $d(x_j)$. In Fig. 3(a), 3(b), $G(m)$ is illustrated for $\beta = 2.5$, $c = 0.3$, $d(x_j) = 10$ and $d(x_j) = 15$ respectively. For example, when $d(x_j) = 15$, $M = 15$ for $\alpha = 3$, $M = 4$ for $\alpha = 4$, and $M = 3$ for $\alpha = 5$, as shown in Fig. 3(b).

3 NUMERICAL RESULTS

In this section we provide numerical results for the impact of the five parameters α, β, γ, c, and $d(x_j)$ on the probability of successful reception $P(x_j)$. In the case of the node degree $d(x_j)$, it is important to note that we manipulate it by changing the respective node density ρ (see Eq. (8)). Of course, *for a fixed number of network nodes* $d(x_j)$ is dependent on the card reception threshold β and path loss exponent, α. Yet, since from the MAC perspective it is the number of node neighbors that are more relevant, we choose to depict the various plots as a function of node degree, even though it is always implied that the respective degree is determined by choosing the node density accordingly.

3.1 Model sensitivity to transmission probability, γ

For fixed α, β, the communication range is also fixed. As long as c remains fixed, the radii of the interference areas and the sizes of interference zones do not change. Nevertheless, the number of nodes in each zone, under uniform node distribution in space, increases linearly with the node density, and thus with the node degree also (Eq. (10)). For a given node degree value, increase of γ implies more communication-active nodes. Higher values of both node degree and transmission probability result in higher loss probability, as intuitively expected.

Figure 4(a) plots the successful reception probability $P(x_j)$ as a function of the node degree for various values of the transmission probability γ. All other parameters are kept constant; the specific values, *i.e.*, $\alpha = 3.84$, $\beta = 2.5$, $c = 0.5$, were chosen so that they match the values measured in the testbed and reported in Section 4. The decrease of successful reception probability is more dramatic for higher node degree values, since the number of potential interfering nodes is then higher. One order size increase of γ, from 0.005 to 0.05 reduces $P(x_j)$ by approximately 13% for $d(x_j) = 30$, versus less than 4% for $d(x_j) = 10$. As a final note, γ in these examples corresponds to an unsaturated network (see discussion in Section 2.2).

3.2 Model sensitivity to path loss exponent, α

The path loss exponent α models the reduction of the radio signal power as a function of distance from the transmitting source. Its values depend strongly on the radio propagation environment [13]. Combining Eq. (2) and Eq. (3) we could write for the radius $r_{j,m}$ of interference area $C_{j,m}$

$$r_{j,m} = \sqrt[\alpha]{m \cdot \beta} \cdot \sqrt[\alpha]{\frac{P_w}{N \cdot \beta}} = \sqrt[\alpha]{m \cdot \frac{P_w}{N}} \qquad (14)$$

As α increases, the signal attenuation with distance is higher and the radii of the interference zones decrease. Nodes can be placed closer to the receiver without interfering with the intended signal. The impact of the parameter α on $P(x_j)$ is plotted in Fig. 4(c). As with Fig. 4(a), higher node degree values amplify the variation of $P(x_j)$ with α.

3.3 Model sensitivity to reception threshold, β

The reception threshold β determines when a MAC frame is successfully received. It depends on the transmission rate, frequency, and sensitivity of the network card/chipset; higher rates and lower-quality network cards require higher β value for achieving a given frame error

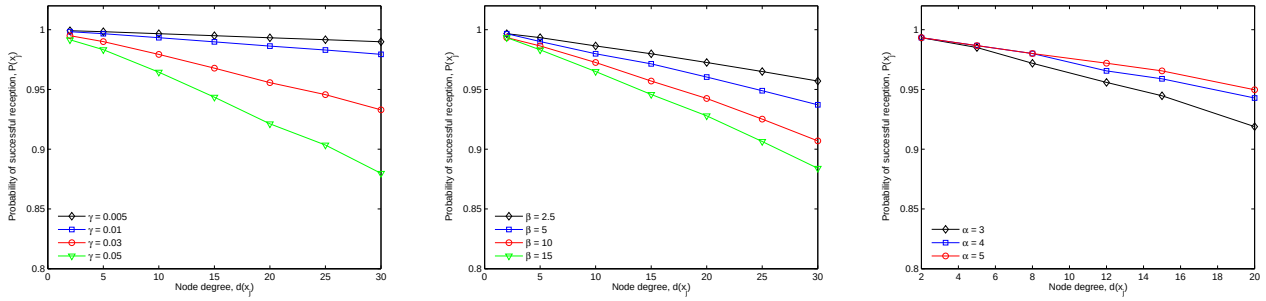

(a) Variable γ, $\alpha = 4$, $\beta = 2.5$, $c = 0.5$. (b) Variable β, $\alpha = 4$, $\gamma = 0.02$, $c = 0.5$. (c) Variable α, $\beta = 2.5$, $\gamma = 0.04$, $c = 0.5$.

Figure 4. Probability of successful reception versus node degree (*i.e.*, node density ρ) for variable γ, β, and α

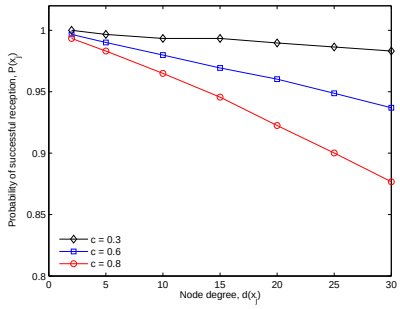

Figure 5. Probability of successful reception versus node degree (*i.e.*, node density ρ) and sender receiver distance c; $\beta = 2.5$, $\alpha = 3.84$, $\gamma = 0.02$

rate. Typical values for β, as reported in network card specifications, are 2.5 to 25 [14].

Increase of the reception threshold value at a given environment reduces the communication range, after Eq. (2), increases the widths of interference zones, as (3) suggests, and for given c results in higher concentration of nodes at the first interference zones, see Eq. (9). The result is increased interference, as shown in Fig. 4(b). The relative reduction on the successful reception probability increases with higher node density, where the concentration of interfering nodes at the first zones becomes more visible.

3.4 Model sensitivity to the sender-receiver distance scale factor, c

In our analytical derivation, we express the distance between the sender and receiver nodes as a ratio of the maximum communication range, $c \cdot r_{max}$. The impact of the sender-receiver distance on the probability of the successful reception is plotted in Fig. 5. We vary the node degree, while letting all other parameters constant. As with α and β, higher network densities magnify the effect of c. Only the latter is more dramatic in absolute terms than the one α and β have on the probability of successful reception.

Finally, Fig. 5 directly points to the well known inefficiencies of minimum-hop routing. Minimum-hop routing tends to select few but distant hops when selecting network routes. This trend results in more noisy but also, as Fig. 5 suggests, more interference-prone links. Of course, "shorter" links may also imply a large number of hops, which can also be detrimental to throughput [5]. Interference-aware routing has benefits in this context and, as explained in Section 4.4, it is an area where our model can find direct application.

4 Model validation via testbed experimentation

The analysis in Section 2 is carried out for a generic MAC-interference model. Yet, real-world MAC protocols bear a large number of finer engineering details, which cannot be easily captured into a simple analytical model without making a much larger number of restrictive assumptions. Therefore, we resort to experimentation to get a better understanding of the strengths and limitations of our analysis in a real wireless network using a real MAC protocol such as the IEEE 802.11b. In what follows, we first present our experimental testbed and describe the experiment configuration. We then, present the experimental results obtained and compare them against the predictions made using our analytical model. Finally, we demonstrate how our model could be used as a metric in an interference-aware routing protocol, and compare the resulting performance against a well-known probe-based routing scheme [15].

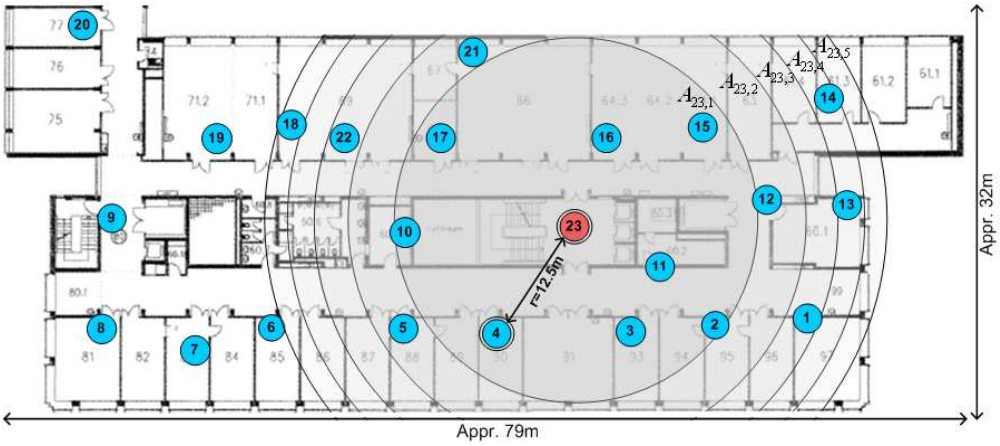

Figure 6. Our wireless mesh network testbed. The 23 802.11a/b/g nodes are distributed in offices all over the floor covering an area of approximately $32x79m^2$.

4.1 Testbed description

The testbed consists of 23 stationary Linux PC nodes equipped with 802.11a/b/g Atheros cards. The nodes are located at the second floor of the ETZ building, as illustrated in Fig. 6. The offices have floor-to-ceiling walls made mostly out of wooden material. All nodes in our testbed communicate using the IEEE 802.11b protocol operating in ad hoc mode. The RTS/CTS handshake mechanism is disabled in line with the default behavior for most wireless cards [16]. The cards are configured to send at 1Mbps with 31.62mW (15dBm) of transmit power.

4.1.1 Path loss exponent α estimation

The dependence of path loss on α is approximated by the log-distance path loss model (*e.g.*, [13]):

$$\overline{P_{ij}}[dBm] = \overline{P_{d_o}}[dBm] - 10 \cdot \alpha \cdot log\left(\frac{d_{ij}}{d_o}\right) \qquad (15)$$

where d_0 is a reference distance, d_{ij} is the distance between the sender i and the receiver j, $\overline{P_{ij}}[dBm]$ is the mean received signal power in dBm and $\overline{P_{d_0}}[dBm]$ is the mean received power at a reference distance d_0. We used two nodes to measure the signal strength as a function of distance in our indoor office environment. The signal strength is derived by the RSS values reported by the cards at various distances. Setting $d_0 = 4m$ and carrying out a least-square fit computation, we estimated $P_{d_0} = -51.12$ dBm, $\alpha = 3.84$. The measured values and the least-square fit curve are plotted in Fig. 7(b).

4.1.2 SINR threshold β estimation

The CMU wireless channel emulator [17] was used to estimate the SINR threshold β of our Atheros wireless cards. In our experiment, two Atheros cards similar to the ones in our testbed, were connected to the hardware emulator; one card was sending 5000 802.11 broadcast packets at 1Mbps and the other was receiving them. Note that 802.11 broadcast packets are not subject to MAC retransmissions. Varying the attenuation of the radio signal through the emulator in increments of 1dB, we estimated β by measuring the ratio of the correctly delivered packets as a function of the received signal strength (RSS). The results are plotted in Fig. 7(a). Since the noise floor of the Atheros cards was measured to be approximately -96dBm, the knee of the delivery ratio curve at RSS =-92dBm means that the threshold value β equals 4dB or 2.5.

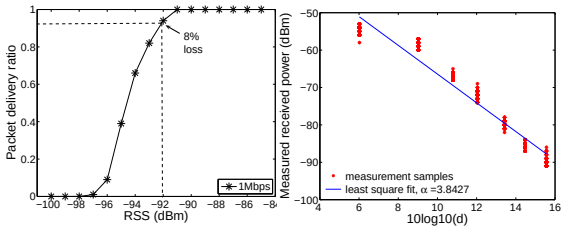

(a) (b)

Figure 7. (a) Packet delivery ratio as a function of signal strength. (b) Signal strength $\overline{P_{ij}}[dBm]$ as a function of the distance d_{ij}.

4.2 Experimentation methodology

The communication range in our testbed for 15dBm of transmit power was measured approximately to 25m. The sender-receiver pair used in our experimental evaluation are

Table 2. Number of nodes in each interference area $A_{j,m} \forall\, m = 1, 2...5$.

$d(x_j)$	$n(A_{j,1})$	$n(A_{j,2})$	$n(A_{j,3})$	$n(A_{j,4})$	$n(A_{j,5})$
5	3,16	12	1	14	
6	11,16	12	1	14	18
7	3,10,16	12	1	14	18
8	3,10,16	5,12	1	14	18
9	3,10,16,17	5,12	1	14	18
10	3,10,11,16	5,12	1	14	18
11	3,10,11,16	5,12	1,22	14	18
12	3,10,11,16,17	5,12	1,22	14	18
13	3,10,11,16,17	5,12,21	1,22	14	18
14	2,3,10,11,16,17	5,12,21	1,22	14	18
15	2,3,10,11,16,17	5,12,21	1,22	14,13	18

nodes 4 and 23, respectively. Their Euclidean distance is $r = 12.5m$, which corresponds to a distance scale factor value of $c = 0.5$.

4.2.1 Distribution of nodes

For the α and β values estimated earlier in Section 4.1, the radii of interference areas for the receiver node 23 using lemma 1 are: $r_{23,1} = 15.8$m, $r_{23,2} = 19$m, $r_{23,3} = 21.1$m, $r_{23,4} = 22.8$m, and $r_{23,5} = 24.1$m. Equations (12)-(13) provide the number of interference areas that have to be considered and Eq. (10) yields the expected number of nodes $E(A_{j,m}) \forall\, m = 1, 2, 3...M$ in each interference zone as a function of the degree of the receiver node 23. We vary the network density by letting the node degree $d(x_j)$ take values in the interval [5,15] nodes. This is done by activating the nodes for each scenario listed in Table 2.

4.2.2 Traffic model description

All nodes in each experimental scenario send IEEE 802.11 broadcast packets, since they involve no retransmissions or link-layer acknowledgments. This is a common practice in related work [6, 7, 18]. We estimate the successful reception probability under simultaneous interfering transmissions measuring the ratio of the successfully received packets over the total number of broadcast packets sent. All experiments were done during the night to circumvent interference induced from external energy sources. Having estimated the parameters α, β and c for our experimental evaluation, we conduct experiments for different network loads.

4.2.3 Node transmission probability γ estimation

The node transmission probability γ in the analysis of Section 2 does not have a direct equivalent in the IEEE 802.11 MAC. To get the equivalent packet send rate for our experiments, we approximate the transmission probability γ of each node as the ratio of the time taken by a successful packet transmission over a large time interval T. Table 3 lists the parameter values used for the basic DCF access mode. Let $H = PHY + MAC + IP + UDP$ be the packet header, Pkt the packet payload and t_{prop} the propagation delay. In the basic access mode, the duration of a successful transmission T_s is

$$T_s = \frac{H+Pkt}{channel\ bit\ rate} + DIFS + E(b) + t_{prop}$$

Let n_{total} the total transmitted packets in time T, then the parameter γ is approximated as

$$\gamma \backsimeq \frac{n_{total} \cdot T_s}{T} \tag{16}$$

Table 3. Parameter values used for the computation of the IEEE 802.11b-equivalent γ parameter

packet payload	128 bits
UDP header	64 bits
IP header	160 bits
LLC+MAC header	192 bits
PHY header	192 bits
Channel bit rate	1 Mbps
Propagation delay	1 μs
DIFS	50 μs
Expected mandatory back-off time E(b)	310 μs

4.3 Experimentation results

In this section, we present our experimental results. All captured traces of this evaluation are available in [19]. We plot average values of the successful packet receptions along with their 90% confidence intervals.

The model predictions are compared against the experimental results in Fig. 8(a)-8(c). We quantify the accuracy of our model by computing the root mean square error (RMSE), defined over the total number k of predictions as $\sqrt{\frac{\sum(est_i - actual_i)^2}{k}}$. There is close match between the two curves in all three figures, the analytical one obtained from the *Interference-cum-MAC* model and the one from the testbed. The analytical predictions for the probability of successful reception match the monotonic change of $P(x_j)$ with the node degree throughout the [5..15] range of node degree values for different γ. This is also reflected in the RMSE values. For $\gamma = 0.005$, the RMSE is 0.025 and for higher $\gamma = 0.05$ the RMSE equals 0.029.

Furthermore, we compare our model with the general model for interference (GMI) proposed in [7]. The model, which reflects the state-of-the-art in interference modelling,

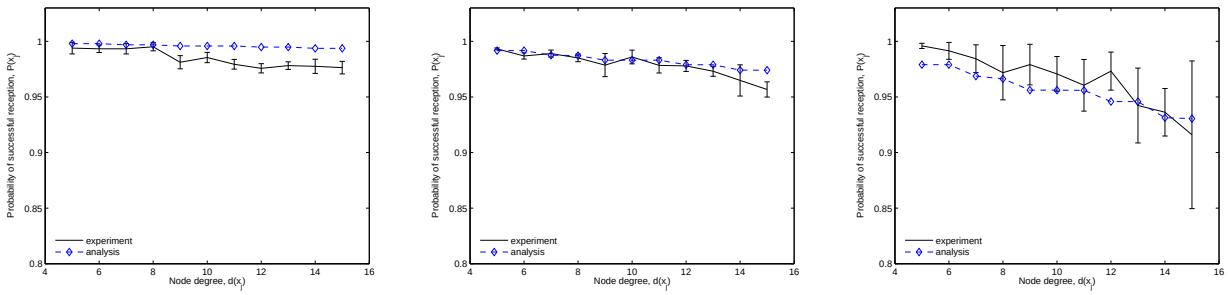

(a) $\gamma = 0.005$, RMSE=0.025. (b) $\gamma = 0.02$, RMSE=0.012 (c) $\gamma = 0.05$, RMSE=0.029

Figure 8. Analytical model *vs.* testbed experimentation results. The analytical model values are $\alpha = 3.84, \beta = 2.5, c = 0.5$

Table 4. Relative error δ in prediction

	$d(x_j)$				
γ	5	6	7	8	
0.005	0.01	0.01	0.005	0.005	Ours
	0.001	0.001	0.001	0.001	GMI
0.02	0.009	0.006	0.005	0.005	Ours
	0.012	0.009	0.009	0.01	GMI
0.05	0.025	0.035	0.035	0.045	Ours
	0.055	0.05	0.05	0.05	GMI

uses measurements to RF-profile the network node and links and then inputs those profiles to MAC models for the analytical derivation of the packet loss probability. The GMI evaluation in [7] was limited to five simultaneous broadcast senders. Here, we compare the predictions of our model and GMI in scenarios of Table 2 involving up to nine simultaneous broadcast senders under unsaturated traffic demands. Note here that the computational time required for the GMI model predictions does not scale with high number of nodes.

Table 4 illustrates the relative error in prediction, $\delta = \frac{abs(est_i - actual_i)}{actual_i}$, for node degree $d(x_j) = [5..8]$. In these scenarios, both models yield comparable accuracy in predicting the measured probability of successful delivery. Interestingly, our model appears to even outperform GMI for higher values of γ (i.e. $\gamma = 0.05$). Moreover our model features distinct advantages over GMI; it is simple, it does not require seed measurements (RF profiling) and is directly applicable to routing, as discussed below.

4.4 Interference-aware Routing

In this section we demonstrate the utility of our model for interference-aware routing protocols. As a proof-of-concept scenario we have enhanced the DSDV protocol with an interference-aware routing metric based on our analytical model and we compare its performance against the Expected Transmission Count (ETX) metric [15] and the minimum hop routing. Due to space limitation, we only discuss the essential elements of our evaluation. Additional plots and discussion about our implementation can be found in [20].

The essential advantage of our analytical derivation is that the probability of successful reception depends on parameters that are available or can be estimated locally at each node. The path loss exponent α depends on the environment, while the SINR threshold β relates directly to the receiving sensitivity of the wireless adapter. The node degree can be known from the state of conventional routing protocols, whereas the network load parameter γ can be estimated by sensing the wireless channel. Modern wireless adapter drivers, such as the madwifi ones [21], permit access to information about the time intervals during which the wireless medium is sensed busy. Finally, the distance r can be available through GPS [22] or other positioning methods. Thus, our analytical expression for the probability of successful reception can directly be used as an interference metric that requires no additional measurements (*i.e.*, probing).

In our implementation of the routing metric, each node distributes its own local estimate of the probability of successful reception $P(x_j)$. To avoid additional overhead in the network, the metric information is encapsulated in the routing packets sent periodically to maintain the routing tables at each node. Then, similar to ETX, each sender node estimates the expected number of retransmissions to a potential receiver neighbor node as $1/P(x_j)$. The routing protocol select paths with the lowest number of retransmissions.

We run experiments in our test-bed for all node pairs, *i.e.*, a total of 23x22=506 pairs. Parameters α, β as well as the distance of nodes are known and the node degree $d(x_j)$ is directly retrieved from the DSDV protocol. Pa-

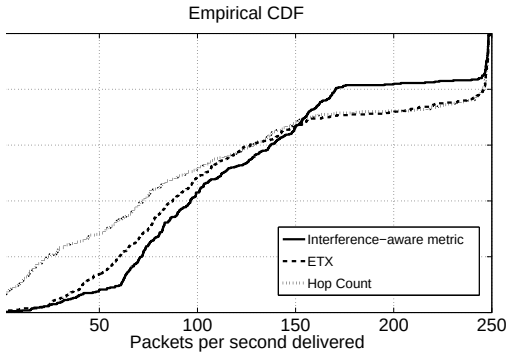

(a) 1Mbps, P_w=10dBm, 128-byte packets.

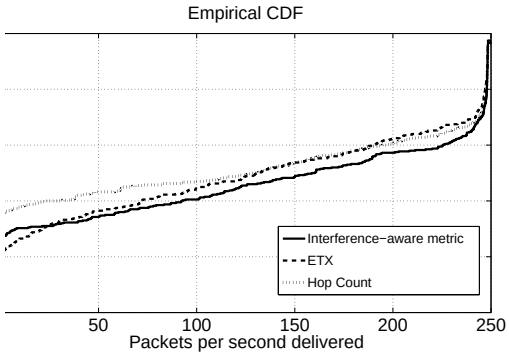

(b) 11Mbps, P_w=10dBm, 128-byte packets.

Figure 9. Throughput CDFs (in packets per second) of paths found by DSDV using ETX, minimum hop-count and our interference-aware metric

rameter γ is estimated in real time at each node similarly to Eq. (16). The wireless medium busy time periods of all received packets are reported in real time from the wireless adapter driver[2]. Figure 9(a) compares the throughput CDFs (in packets per second) of paths found by DSDV using ETX, minimum hop-count and our interference-aware metric. Our metric as well ETX select higher throughput paths than hop count. Similar behavior can be observed also in the second scenario for 11Mbps transmit rate, as shown in Fig. 9(b). These results exhibit the utility of our model as a metric for interference-aware routing, while avoiding probe measurements.

5 Related Work

Multiple access interference has always been one of the main concerns when building wireless networks. Whereas its impact is quite well understood and addressed in infrastructure-based cellular networks (see, for example, [23] and [24]), its characteristics and impact in multihop networks are less well understood.

Jain *et al.* in [2] propose the use of conflict graphs for describing interference between neighboring nodes. Contrary to the typical graph semantics, vertices of the graphs are the individual network links(hops) with an edge connecting them when the two links interfere. The authors use this abstraction to derive bounds for the optimal network throughput under ideal routing and scheduling decisions but they do not propose any way to derive the conflict graph. This was addressed in [18] and [6]. Padhye *et al.* in [18] use broadcast transmissions to derive the Broadcast Interference Ratio (BIR) as a measure of the interaction between two network hops, whereas Reins *et al.* combine a simplified analytical model for the CSMA/CA function of 802.11 with fewer measurements (n versus n^2 in [18], where n the number of network nodes) to estimate BIR values and determine the graph edges [6]. While their model is limited to two competing broadcast senders, Qiu *et al.* develop a general interference model for arbitrary number of senders [7]. Both models have as starting point RSSI measurements that profile the network nodes and become inputs to the analytical model. On the contrary, our approach is fully analytical and circumvents the need for measurements and their pitfalls, such as the limited accuracy of the reported RSSI values and their inappropriateness for non-static networks.

In a different line of work, focusing more on protocol engineering, there is agreement in the research community that interference should be an input for routing protocols. Several routing metrics have been proposed to overcome the inefficiencies of minimum-hop routing; they rely on estimation of the path round trip time (RTT), expected data transmission count (ETX) [3], and the weighted cumulative expected transmission time (WCETT) [4] to drive routing decisions. The main disadvantages of these approaches is that they rely on probe measurements. Besides the overhead they impose on the network, they suffer from inaccuracy and limited responsiveness to network node mobility. Interference-aware routing is an area where our analytical derivation can have direct application, in the same time avoiding the pitfalls of the measurement-based approaches.

6 Conclusions

Our paper addresses interference in ad hoc wireless networks. Starting from the SINR model, we derive an analytical expression for the data loss probability as a function of the network density, load, propagation environment, and network card hardware. The analysis is carried out assum-

[2]For this, we modified the Madwifi wireless adapter drivers [21] to report the duration of each packet.

ing a MAC-agnostic model, which does not take into account the engineering details of real-world protocols, such as the IEEE 802.11x suite of protocols. We then extend our analytical derivation with a simple enhancement to capture the carrier sense function of real-world MAC protocols. To assess the prediction capacity of our analysis under realistic conditions, we have set up a wireless mesh network testbed. Measurements obtained from the testbed show close match between the analytical predictions and experimental results.

Where and how could this analytical derivation be useful? Interference-aware routing is one profound area. The analytical derivation could eventually evolve to a routing metric used by routing protocols to route packets in the network. This is indeed promising, since it results in significant control data overhead savings over state-of-the-art measurement-based approaches in the literature. As a proof-of-concept scenario, we have implemented an interference-aware routing metric based on our analytical model and we show that its performance compares favorably with the ETX metric, without the need for active probe measurements. In general, an interference-aware routing metric using our analytical model can be refined and tailored according to the specific objectives of the routing algorithm, such as robustness, scalability, low latency, high throughput, or energy efficiency.

References

[1] IEEE. IEEE 802.11. *IEEE Standards for Information Technology*, 1999.

[2] K. Jain, J. Padhye, V. Padmanabhan, and L. Qiu. The impact of interference on multi-hop wireless network performance. In *Proc. MobiCom '03*, San Diego, CA, USA, September 2003.

[3] D. S. J. De Couto, D. Aguayo, J. Bicket, and R. Morris. A high-throughput path metric for multi-hop wireless routing. *Wireless Networks*, 11(4):419–434, July 2005.

[4] R. Draves, J. Padhye, and B. Zill. Routing in multi-radio, multi-hop wireless mesh networks. In *Proc. MobiCom '04*, Philadelphia, PA, USA, September 2004.

[5] P. Gupta and P.R. Kumar. The capacity of wireless networks. *IEEE Trans. on Information Theory*, 46(2):388–404, March 2000.

[6] C. Reis, R. Mahajan, M. Rodrig, D. Wetherall, and J. Zahorjan. Measurement-based models of delivery and interference in static wireless networks. In *Proc. SIGCOMM*, Pisa, Italy, September 2006.

[7] L. Qiu, Y. Zhang, F. Wang, M. K. Han, and R. Mahajan. A general model of wireless interference. In *Proc. MobiCom '07*, pages 171–182, New York, NY, USA, 2007.

[8] G. Bianchi. Performance analysis of the IEEE 802.11 distributed coordination function. *IEEE Journal on Selected Areas in Communications*, 18(3):535–547, March 2000.

[9] A. Kumar, E. Altman, D. Miorandi, and M. Goyal. New insights from a fixed point analysis of single cell IEEE 802.11 WLANs. In *Proc. INFOCOM 2005*, Miami, FL, USA, March 2005.

[10] Mathworld. http://mathworld.wolfram.com/circle-circleintersection.html.

[11] G. Pesta C. Bettstetter and P. Santi. The node distribution of the random waypoint modility model for wireless ad hoc networks. *IEEE Trans. on Mobile Computing*, 2(3):257–269, July-September 2003.

[12] P. Naina, D. Towsley, B. Liu, and Z.Liu. Properties of random direction models. Technical Report RR-5284, INRIA, July 2004.

[13] T. S. Rappaport. *Wireless Communications: Principles and Practice*. Prentice Hall PTR, 2nd edition, 2001.

[14] Cisco Aironet 802.11a/b/g Wireless CardBus Adapter datasheets.

[15] D. S. J. De Couto, D. Aguayo, J. Bicket, and R. Morris. A high-throughput path metric for multi-hop wireless routing. In *Proc. MobiCom '03*, San Diego, CA, USA, September 2003.

[16] M.Gerla K. Xu and S. Bae. Effectiveness of RTS/CTS handshake in IEEE 802.11 based ad hoc networks. *Ad Hoc Networks Journal*, 1(1):107–123, July 2004.

[17] G. Judd and P. Steenkiste. Using emulation to understand and improve wireless networks and applications. In *Proc. 2nd NSDI*, pages 203–216, Berkeley, CA, USA, May 2005.

[18] J. Padhye, S. Agarwal, V. Padmanabhan, L. Qiu, A. Rao, and B. Zill. Estimation of link interference in static multi-hop wireless networks. In *Proc. Internet Measurement Conference (IMC) 2005*, Berkeley, CA, USA, October 2005.

[19] Computer Engineering and Networks Lab. www.csg.ethz.ch/people/parissidis/experimental-evaluation/.

[20] G. Parissidis, M. Karaliopoulos, T. Spyropoulos, M. May, and B. Plattner. An interference-aware routing metric for wireless multi-hop networks. Technical Report 279, Computer Engineering and Networks Laboratory, ETH Zurich, December 2007.

[21] Madwifi website. www.madwifi.org.

[22] M. Moeglein Z. Biacs, G. Marshall and W. Riley. The Qualcomm/SnapTrack wireless-assisted GPS hybrid positioning system and results from initial commercial deployments. In *Proc. Institute of Navigation(ION) Conference 2002*, Portland, OR, USA, September 2002.

[23] D. Tse and P. Viswanath. *Fundamentals of Wireless Communications*. Cambridge University Press, UK, 2005.

[24] William C. Y. Lee. *Mobile Communications Engineering*. McGraw-Hill Telecommunications, NY, USA, 2nd edition, 1998.